Study and Characterization of the Substrate and Thin Film of the ZrO_2-Y_2O_3/Al_2O_3 Solid Oxide Fuel Cells

M. Reyes-Reyes[1], J. Reyes-Gasga[1], Jong-Wan Park[2] and You-Kee Lee[2]

[1]Instituto de Física, UNAM. Apdo. Postal 20-364, 01000 México D.F., México.
[2]Dept. Of Metallurgical Engineering, Hangang University, 17 Haengdangdong, Seongdong-Ku, Seoul 133-791, Korea.

Abstract

The structural and chemical characterization of the substrate and thin film of the zirconia-ytria/alumina system for Solid Oxide Fuel Cells and their electrical conductivity behaviour are presented in this work. As a result of sputtering-radio-frequency deposition onto a porous alumina substrate, very homogeneous thin films of zirconia-ytria were produced. These nanograined thin films did not show any fracture or hole and its atomic structure was identified as the zirconia monoclinic phase. The substrate showed two alumina phases: corundum and alpha-alumina. All the samples exhibited a good electrical conductivity with slight variations in the range of temperature from 573 to 1173°K.

Introduction

Since the discovery of fire and its uses, man has began the search for several energy sources. One of them was the Voltaic battery where the chemical energy is transformed into electrical. Actually, the research on fuel cells promises to be an attractive alternative to other modes of energy sources. Fuel cells offer several advantages over another types of batteries: substantially higher conversion efficiency, high efficiency at partial load, minimal sitting restriction, potential for co-generation and much lower production of pollutants (Appleby, 1994; Steele, 1994).

Fuel cells work in the reverse way of the water electrolysis. The most simple fuel cells use hydrogen as fuel and oxygen as oxidant. In this process, the oxidant is fed to the cathode where is reduced and the fuel is fed to the anode where is oxidized. The electrolyte carries ions between the two electrodes. The electron flow between the anode to the cathode produces direct electrical current.

The most successful type of cell used for static applications is the SOFC (Solid Oxide Fuel Cell). SOFCs presents many advantages over the other types of fuel cells: the use of a solid electrolyte avoid problems of corrosion and handling, they can be produced in very thin layers and the cell components can be molded into unique shapes unachievable for fuel cells having a liquid electrolyte. Evenmore they are the best candidates for industrial and domestic uses because they have a good chemical stability at high temperature, high potency, do not present polarization in its electrodes, are easy to manage, and their lifetime is of twenty or more years.

The development of SOFCs has been profited for the research of new materials to be used as solid electrolyte and electrodes, and the development of new techniques for its fabrication. One of the principal advantages of using thin films in SOFC is that the ohmic resistance of the electrolyte decrease and its temperature of operation is maintained in range from 873 to 1073°K. This eliminates the gas problems of interconnection and sealing.

Some solid oxide fuel cells can now present parameters of 0.7 Volts at 200 mA/cm^2 with 85% of efficiency (Appleby, 1994). Up to now the unique practical solid oxide electrolyte successfully used is ytria stabilized zirconia (YSZ) because of its lower cost, high conductivity and no contamination. The performance of SOFCs depends greatly on the electrical properties of the YSZ electrolytes. However, YSZ films are somewhat difficult to fabricate because they need to be gas tight, sufficiently thin and mechanically stable. It has been commented that a better conductivity is obtained with YSZ thin film of the order of 10nm in thickness (Barnet, 1990), but this is still a point of discussion.

An important point in the production of SOFCs is to have an adequate technique of thin film deposition in such a way that the substrate could be at low temperature while high velocities of deposition is in process. Comparing the chemical vapor deposition (CVD) and the physical vapor deposition (PVD), CVD is generally utilized for deposition of films for SOFCs with thickness of 50nm (Carolan and Michaels, 1987), but it requires generally a high temperature in the

substrate (1073^{0}K) in the conventional case. In the PVD methods, the deposition of radio-frequency (RF) magnetron sputtering is more utilized for the production of YSZ thin films. This technique permits, an excellent control over the thickness, structure, intrinsic strength adhesion and composition of the film (Greene et al., 1976; Thiele et al., 1991).

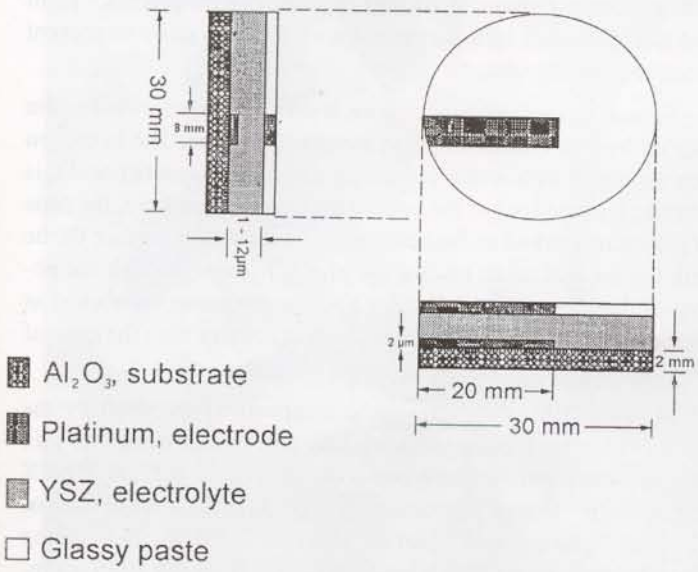

Fig. 1: *Schematic representation of the SOFC´s components and sizes according with the manufacturing sequence.*

In this work RF magnetron sputtering YSZ thin films were deposited on porous alumina substrates and the structural and chemical characterization of the substrate and thin film and their electrical conductivity behaviour are presented. For structural and chemical characterization transmission (TEM) and scanning (SEM) electron microscopy together with electron diffraction, energy dispersive spectroscopy of characteristic x-ray (EDS) and x-ray diffraction (XRD) analyses were used. The complex impedance technique was used for electrical conductivity measurements of the samples.

Experimental Procedure

Porous alumina substrates were prepared from alumina powder (Alcoa Al6AG), ball milling it with isopropyl alcohol for 24h in a plastic jar and dried for 48h at 353^{0}K. Afterwards this powder was crushed and unaxially dry-pressed with a pressure of 100Kg/cm^2 using a stainless steel mold of 23 mm in diameter and sintered at 1623^{0}K for 2h.

The sequence for fabrication of the YSZ-SOFC was the following (figure 1). First, platinum (the electrode) was deposited over surface of the porous alumina substrate (a disc of 23mm in diameter and 2mm in thickness) forming a rectangle (8mm x 20mm) with a thickness of around 2mm. A film of YSZ of approximately 1mm in thickness was deposited by RF magnetron sputtering over this electrode and the

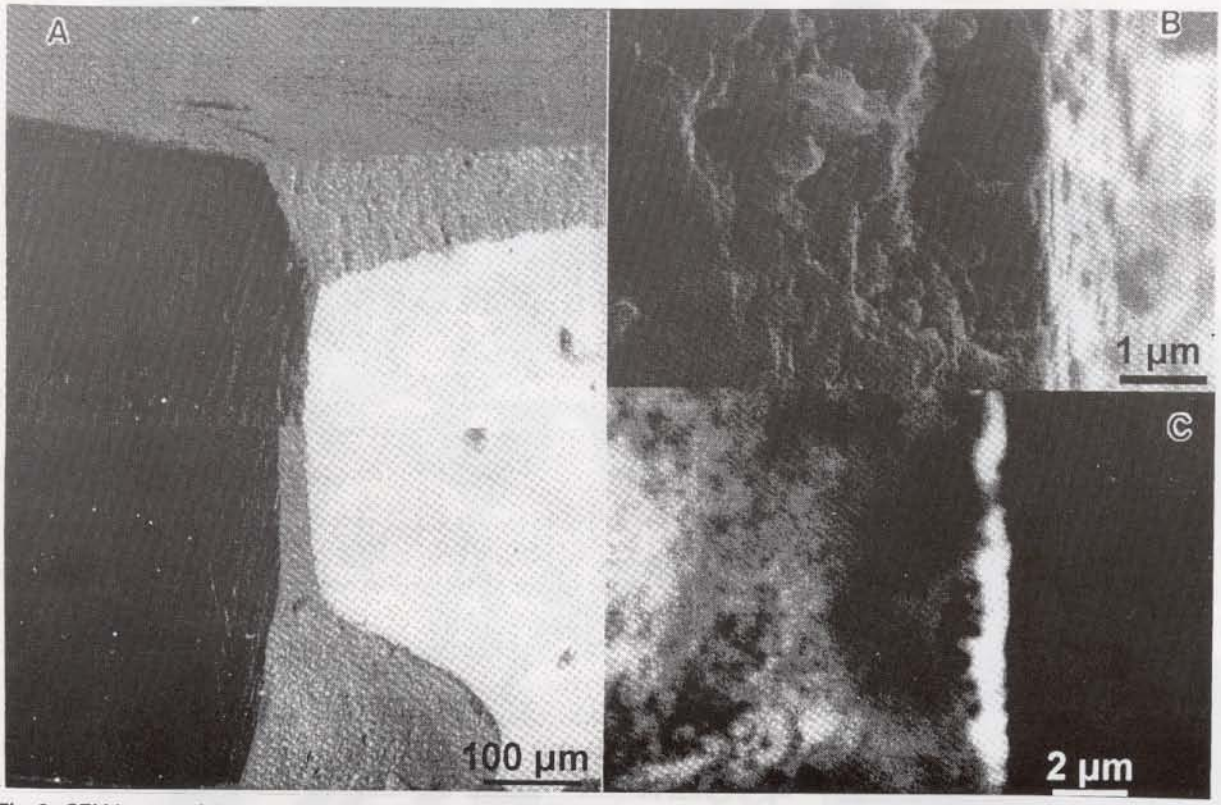

Fig. 2: *SEM images of the sample.* **A:** *General view: the most brilliant face is where the thin film was evaporated.* **B:** *cross section secondary electrons image of the substrate-thin film interface.* **C:** *Backscattering electron image of (B). Note the grained and porosity morphology of the substrate in (B) and the irregularity of the substrate-thin film interface in (C).*

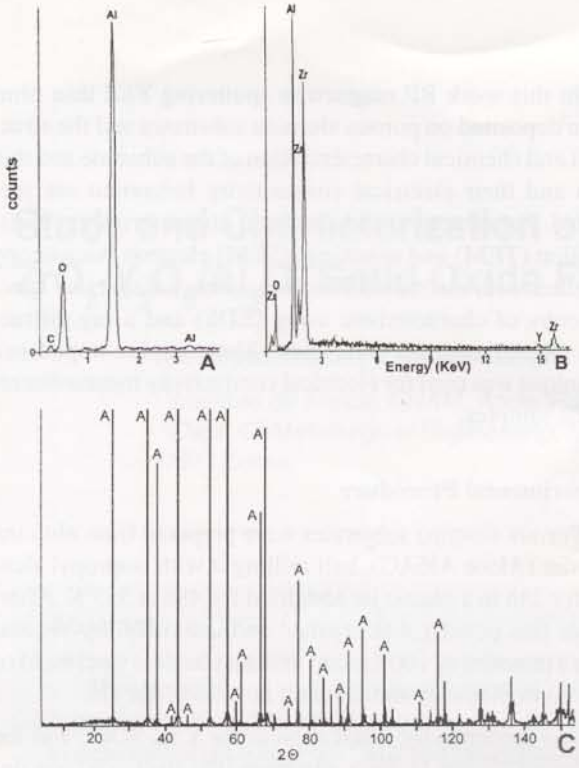

Fig. 3: *X-ray analyses.* **A:** *EDS spectrum from the substrate and* **B:** *EDS spectrum from thin film along the cross section direction.* **C:** *X-ray diffractogram from the substrate. The letter "A" indicates the a-alumina and corundum peaks. The peaks without identification correspond to corundum only.*

remaining surface of the disc. For this, the chamber was pumped down to 5 x 10^{-6} torr before the introduction of sputtering gases and pre-sputtered for 20 min. was carried out to clean the substrate surface before deposition. The sputtering was done for about 2h in an Ar atmosphere of 5 mtorr with a RF power of 4.4 W/cm^2 and deposition rate of 750 nm/h. After deposition, the thin films were annealed at 773^{0}K for 2h. Over the surface of this YSZ thin film a rectangle (8mm x 20mm) is painted with platinum paint and the remaining area is covered with a glassy paste to prevent any unexpected leakage.

To test the fuel cell functioning, it was supported with the film face up by two mullite tubes in a electric furnace. The hydrogen was saturated with water vapour (at room temperature), and this mixture was the fuel of the upper surface of the cell. So, the cape of platinum worked as fuel electrode. In the lower surface of the cell, the air was taken toward the platinum cape through the porous of the substrate and the film YSZ; so the substrate worked as air electrode. A thermocouple was set in contact with the cape of platinum to register the temperature of operation.

For the TEM observation, the sample was prepared by the method of cross section in such a way that the substrate and thin film structures and their interface could be studied. A JEOL 100CX transmission electron microscope was used for these observations. The samples were also observed with the JEOL 6400 scanning electron microscope which has attached an NORAN EDS equip-

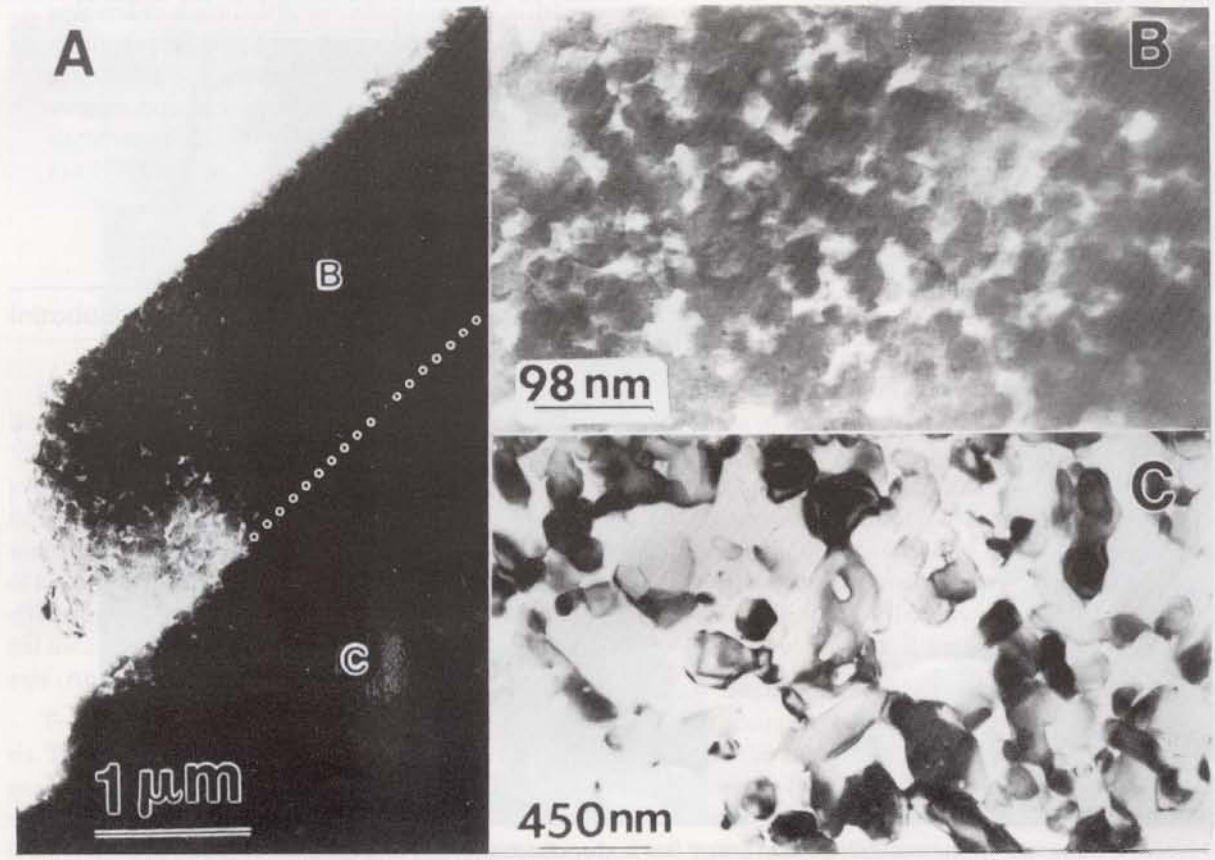

Fig. 4: *TEM images of the substrate-thin film interface.* **A:** *General view: the pointed line indicates the interface position.* **B:** *Bright field image of the thin film.* **C:** *Bright field image of the substrate. Note the difference in grain size in both images.*

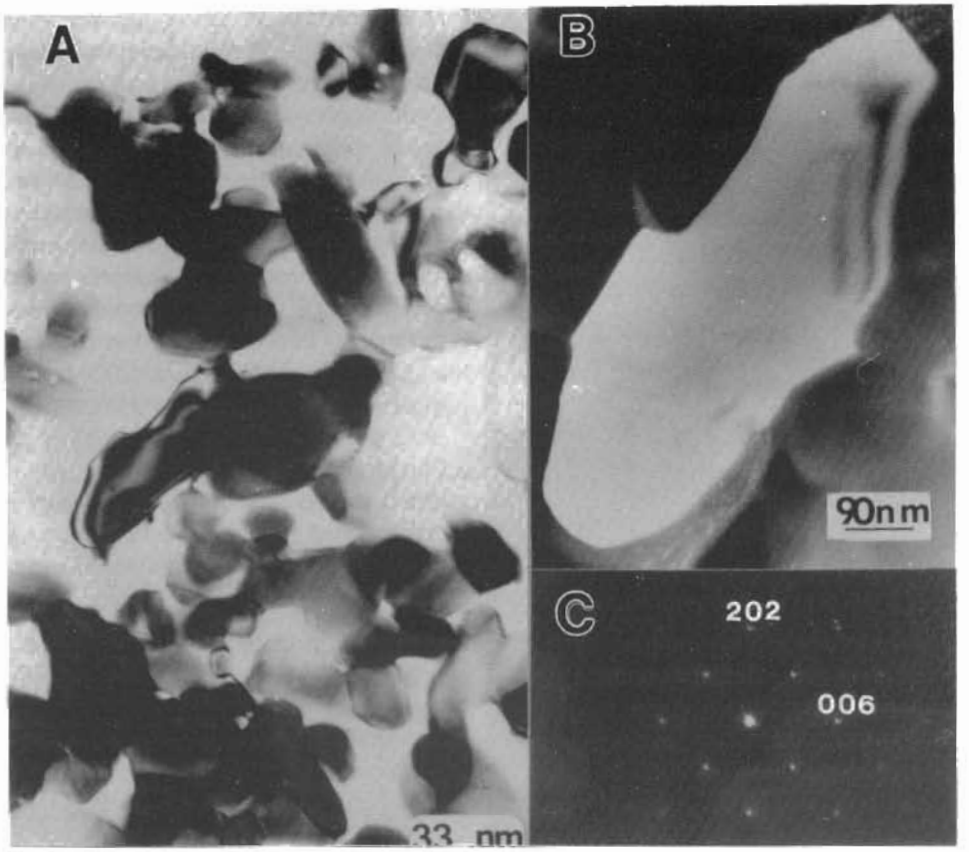

Fig. 5: *TEM images the substrate.* **A:** *General view, a bright field image;* **B:** *dark field image of one of the grains shown in (A); and* **C:** *electron diffraction pattern from the grain shown in (B). The indexation of the diffraction pattern coincides with a rombohedral (hexagonal) unit cell.*

ment for characteristics x-ray analysis. X-ray diffractograms were obtained with the X-ray diffractometer SIEMENS D-500 using CuKa radiation. For electrical conductivity measurements of the samples in the frequency range of 0.1 Hz to 1 MHz, an Schlumberger Technologies impedance analyser, model SI-1255, was used.

Results and Comments

1. SEM and chemical analysis

SEM was used to study the topography of the thin film deposited the substrate. Figure 2a is a general view of the YSZ thin film over the substrate of alumina. In this figure the thin film surface looks very plane, without defects and deformations. In figure 2b the sample is observed close to the cross-section direction in such a way that the substrate-film interface could be observed. This is a secondary electron image and it only shows the granulation of the substrate because the substrate-film interface is not detected. This substrate-thin-film interface is more easily recognised if the image is produced with backscattering electrons because the difference in densities of the substrate and the film (figure 2c). The thickness of the film is approximately 1mm. As it can be observed in last image, the thickness of the substrate-film interface is not constant but variable, because of the granulated substrate; however the film surface is completely flat.

The chemical analysis of the substrate and the thin film was made by techniques of EDS and XRD (figure 3). The identification by EDS of characteristic x-ray spectra (figure 3a), together with the x-ray diffractogram (figure 3c) from the substrate, indicates that its structure corresponds to the alpha-alumina phase and corundum. These both types of alumina have a hexagonal-rombohedral unit cell and spatial group R-3d (No. 167) and their difference in the unit cell parameters is almost insignificant: a = 4.758Å and c = 12.991Å for the corundum and a = 4.759Å and c = 12.991Å for the alpha-alumina. The alpha-alumina phase is the most stable among the types of alumina though it always coexist with the others, in this case with corundum. The thin film presented an average chemical composition of 92% ZrO_2 and 8% Y_2O_3 (figure 3b), that is, the ZrO_2-Y_2O_3 phase.

2. Transmission electron microscope

Figure 4a is a TEM view of the substrate-thin film interface showing the type of crystallinity of the film (figure 4b) and substrate (figure 4c). The average grain size of the film was of approximately 80nm, but the amorphous phase seems to be a majority when it is compared with the crystalline phase. The average grain size in the substrate is approximately 400nm (fig. 4c).

Electron diffraction patterns from the substrate (figure 5) confirmed those of x-ray diffraction: a rombohedral (hexagonal) phase. The thin film presented an electron diffraction pattern of concentric rings whose indexation indicated that it corresponds to the ZrO_2-Y_2O_3 phase with monoclinic unit cell (figure 6). Figure 6b presents the dark field image corresponding to the ring (400) of diffraction pattern shown in figure 6c whereas figure 6d shows the corresponding for the (201) ring. In this case the grains in the thin film are of the order 80nm or smaller in size.

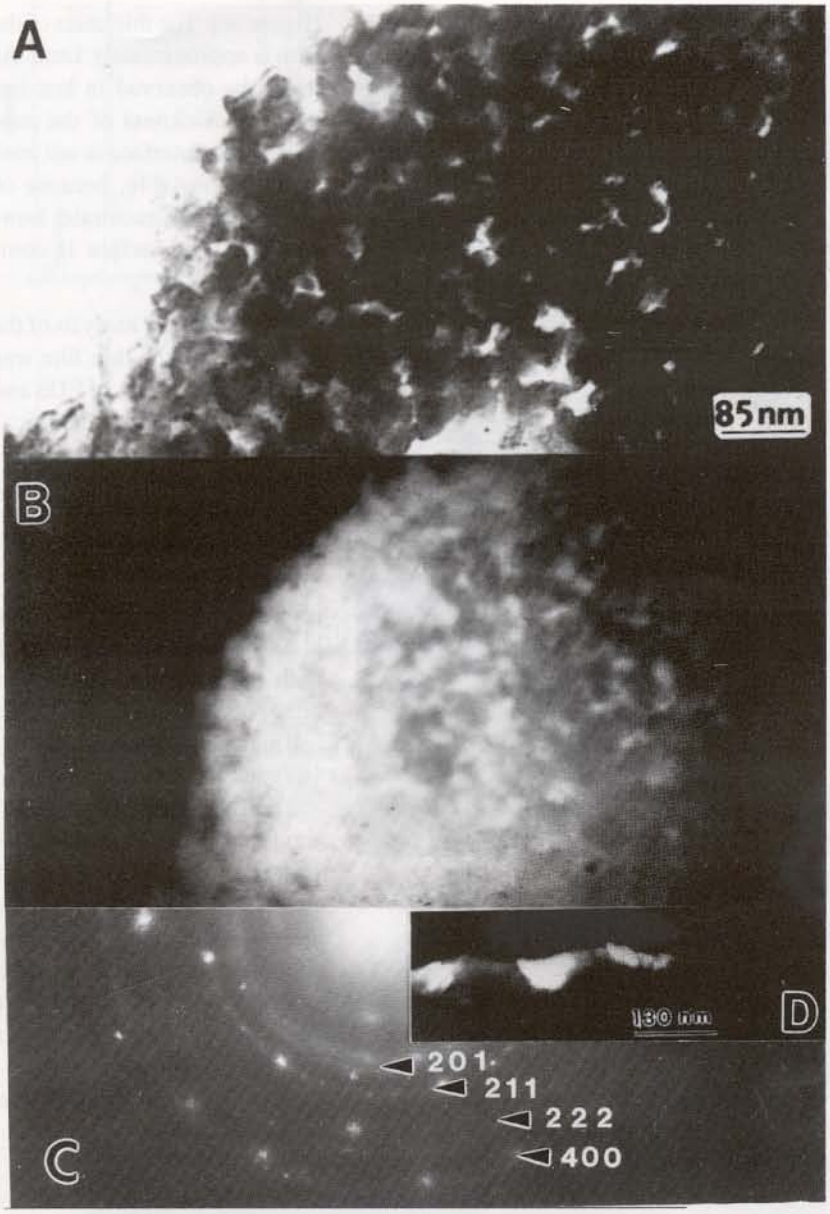

Fig. 6: *TEM images of the thin film. A) General view: bright field image. B) Dark field image formed with the ring (400) of the diffraction pattern exhibit in (C); note the grained structure of the thin film. D) Dark field image with the ring (201) of the diffraction pattern exhibit in (C); note the grain size in this case.*

3. Electrical properties

The conductivity of the sputter-deposited YSZ films was found to be slightly lower than those of bladed YSZ thin plates and dry pressed YSZ pellets reported previously (You-Kee Lee et al, 1997). This difference is due to the electrical conductivity measurement itself and not to the conduction mechanism of oxygen ions through zirconia. That is, the inductance of the relatively long Pt wire connecting specimens to the impedance analyser used for the electrical conductivity measurement is not separable from the total impedance of the thin film so that the electrical conductivity detected can be decreased. Moreover by the experimental arrangement, it is also thought that the high resistance of alumina used as a substrate affects the total impedance.

For all the samples, in the range of temperature from 573 to 1173°K, the electrical conductivity exhibited a slight variations in the temperature dependency (figure 7). The total conductivity containing both bulk and grain boundary contributions was observed to obey the relation:

$$s = A \exp(-E_a / k_B T)$$

where A, E_a and K_B are a pre-exponential coefficient, activation energy for oxygen ion diffusion and the Boltzmann constant respectively. Although, it was confirmed that the contribution of the bulk component to the total electrolyte conductivity of all the samples was larger than that of the grain boundary component (You-Kee Lee et al, 1997).

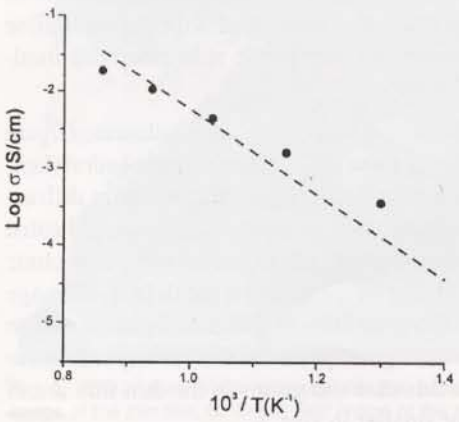

Fig. 7: *Temperature dependence of total conductivity of the sputtered YSZ thin films in the temperature range from 573 to 1173°K.*

Conclusions

We have the following conclusions for the SOFCs developed for the ZrO_2-Y_2O_3/Al_2O_3 according with the experimental procedure here presented. The substrate shows grains of the order 400nm and is slightly porous; porous alumina showed two alumina phases: corundum and alpha-alumina. SEM images showed a film without fractures and grained structure indicating absence of tension strengths and a homogeneous thin film growth. TEM images showed a thin film with a polycrystalline structure, with grain size of

approximately 80nm. The diffraction patterns indicated a monoclinic phase of the YSZ for the crystalline phase which is inside of an amorphous matrix. The absence of porosity in the thin films means a barrier to the fuel transportation such as the air and a better efficiency of the SOFC. The studies of electrical conductivity indicate that this type of structure presents a good conductivity in the range of temperature from 573 to 1173°K. Nevertheless, the yttrium partial stabilised zirconia ceramics presents its better result when it is completely crystalline. Therefore, this conductivity can be improved if the observed amorphous matrix would be reduced. This is only obtained changing the deposition parameters of the thin film.

Acknowledgements

We thanks the technical help received from P. Mexia, C. Flores, R. Hernández, S. Tehuacanero, C. Zorilla and A. Sanchez from IFUNAM; F. Solorio from UMSNH; C. Angeles from ININ. A. Reyes Rojas e Hilda Esparza (CIMAV). This work was economical supported by CONACYT trough project 3271-PA9608.

References

Appleby, A. J. (1994) Fuel cell electrolytes: evolution, properties and future prospects. J. Power Sources. 49: 1-14.

Barnett, A. (1990) Silicon-film solar cell development on ceramic substrates, Proceedings of IX International Conference on Photovoltaic Solar Energy. Freiburg, West Germany 25-29 Sept. 1989. Kluwer Acadamic Publishers. Pags. 697-700.

Carolan, M. F., and Michaels, J. N. (1988) Chemical vapor deposition of ytria stabilised zirconia on porous supports. Solid State Ions Diffus. React. 25: 207-216.

Greene, J. E., Wickersham, C. E., Zilko, J., Welsh, L. B., and Szotran, F. R. (1976) Morphological and electrical properties of rf sputtered Y_2O_3-doped ZrO_2 thin films. J. Vac. Sci. Technol. 13: 72-75.

Steele, B. C. H. (1994). Oxygen transport and exchange in oxide ceramics. J. of Power Sources. 49: 1-14.

Thiele, E. S., Wang, L. S., Mason, T. O., and Barnett S. A. (1991) Deposition and properties of ytria-stabilised zirconia thin films using reactive direct current magnetron sputtering. J. Vac. Sci. Technol. 9: 3054-3060.

You-Kee, L., and Jong-Wan, P. (1997) Microstructure and electrical conductivity of yttria-stabilized zirconia electrolyte thin plates produced by the doctor blade method. J. Mat. Sci. Lett. 16: 678.

Tsai, T., and Barnett, S. A. (1995) Sputter deposition of cermet fuel electrodes for solid oxide fuel cells. J. Vac. Sci. Technol. 13: 1073-1077.